ACOUSTICS 2012

Nearfield acoustic holography in wind tunnel by means of velocity LDV measurements

H. Parisot-Dupuis, F. Simon and E. Piot

ONERA - The French Aerospace Lab, 2 av Edouard Belin, F-31055 Toulouse, France
helene.parisot_dupuis@onera.fr

With the efforts made on environmental noise reduction, aeroacoustic studies in wind tunnel are required to characterize the main sources during airplanes conception. For a long time, beamforming, based on farfield microphone measurements, has been the only method used. Recently, a new method based on Nearfield Acoustic Holography using a convective spectral pressure-to-pressure propagator was tested too (Kwon & al. JASA 2010). This method avoids some errors linked to farfield measurements and allows the integration of convection effects in the propagator without any assumption on sources. However, nearfield microphone measurements are required, which creates flow and measurements disturbances. That is why it is interesting to develop another method allowing wind tunnel aeroacoustic sources characterization by means of non-intrusive nearfield measurements. This paper presents a numerical validation of a new method coupling Nearfield Acoustic Holography based on a convective real velocity-to-pressure propagator with LDV velocity measurements. Simulations in the case of monopoles and dipoles radiating in uniform subsonic flows show a good characterization of sources.

1 Introduction

With the great development of transports, aeroacoustic sources localization on models in wind tunnel is a relevant issue today. For this purpose, array-based measurement techniques have been developed in the 1970s [1], like the acoustic mirror, the acoustic telescope and the polar correlation technique. The acoustic telescope, also called beamforming, is the most used nowadays. This method is based on monopole sources hypothesis and allows acoustic sources localization by means of farfield microphone array measurements. It has been applied to many aeroacoustic problems, for instance localization of sources on moving objects or source localization in open and closed wind tunnel test sections [2]. Nevertheless, for wind tunnel applications, corrections are required to deal with disturbances created by shear layers (open-jet facilities) or boundary layers (closed test sections), wall reflections and acoustic wave convection by the mean flow [3]. In that way, beamforming provides an accurate localization of acoustic sources in wind tunnel conditions, but inverse [4] or time-reversal [5] methods are necessary to obtain amplitudes of acoustic sources.

That is why recent studies show applications of Nearfield Acoustic Holography (NAH) for aeroacoustic sources characterization too. This method, introduced by Williams & al. in 1980s [6, 7], is an other acoustic imaging technique to characterize stationary sound sources without flow. It allows acoustic sources evaluation by reconstructing toward source plane the acoustic field measured on a surface situated in the nearfield of sources, called the hologram plane. As this reconstruction corresponds to an ill-posed inverse problem, regularization methods [8] are usually required to improve the quality of evaluated field. The problem of this method for wind tunnel application is that airflow effects are not integrated in classical NAH procedures.

In order to avoid this problem, Ruhala & al. [9] proposed a NAH procedure applicable in a moving fluid medium at subsonic and uniform velocity. In this method, a new Green's function and modified wave number filter including mean flow effects are proposed and tested numerically. However, this procedure is based on low subsonic Mach number flows approximation.

For the purpose of avoiding this limitation, Kwon & al. [10] have presented recently a NAH procedure for sources radiating in high subsonic Mach number flows. In this work, a mapping function is derived to link the static spectral space to the moving one, giving a new Green's function and wave number filter. Simulations and experiments using a procedure to reduce the corruption of measured signals by microphones-flow interactions show the applicability of the method. However, these experiments were performed at a relatively low Mach number (M=-0.12).

For higher Mach numbers, in-flow microphones array can generate additional noise and disturb the flow pattern affecting reconstructed fields. Thus, the purpose of this paper is to validate numerically a NAH procedure allowing aeroacoustic sources characterization in subsonic wind tunnel based on non-intrusive measurements. The idea developed here is to use LDV (Laser Doppler Velocimetry) velocity measurements to obtain mean and acoustic velocity fields in the hologram plane. To take into account the flow, convective Rayleigh's first integral formula is used to derive convective velocity-to-pressure propagator in real-space [11] contrary to those developped by Kwon & al. [10] that are written in spectral-space.Discrete Fourier transform of this propagator allows then the evaluation of acoustic fields in source plane. To validate this procedure, simulations of high-lift airfoil aeroacoustic sources (monopoles and dipoles) radiating in uniform subsonic flow at various Mach numbers are conducted.

2 Theory

In this section, a brief overview of classical NAH theory is presented (for more details see [6, 7]) in order to introduce NAH in moving fluid medium. As the aim is to apply NAH from LDV velocity measurements, the following is focused on velocity-to-pressure propagators. The potentiality of velocity-based NAH without mean flow has already been tested by Jacobsen & al. [12] with the development of particle velocity transducers called "Microflown".

2.1 Velocity-based NAH in static fluid medium

Classical velocity-based NAH theory for a fluid medium at rest is based on the first Rayleigh's integral formula [6]. For a cartesian coordinate system, this formula links acoustic pressure at $\mathbf{r} = (x, y, z)$ to normal acoustic pressure gradient on surface $S = (x', y', z')$ using Neumann Green's function G_N:

$$p(\mathbf{r}, \omega) = -\iint_S G_N(\mathbf{r} \mid \mathbf{r}', \omega)\, \partial p(\mathbf{r}', \omega)/\partial z\, dx'dy' \qquad (1)$$

$$\text{with} \begin{cases} G_N(\mathbf{r} \mid \mathbf{r}', \omega) = e^{ikR}/2\pi R \\ R = \mid \mathbf{r} - \mathbf{r}' \mid = \sqrt{(x - x')^2 + (y - y')^2 + (z - z')^2} \end{cases}$$

where k is the wavenumber, ω is the angular frequency and $i = \sqrt{-1}$.

Using Euler's equation normal pressure gradient can be expressed in terms of normal particle velocity u_z:

$$\partial p(\mathbf{r}',\omega)/\partial z = i\rho\omega\, u_z(\mathbf{r}',\omega) \qquad (2)$$

where ρ is the density of fluid medium.

As two-dimensional convolution product corresponds to a simple multiplication in spectral space, NAH uses two-dimensional spatial Fourier transform of Eq. (1):

$$p(\mathbf{r},\omega) = \mathcal{F}^{-1}[-i\rho\omega\, \mathcal{F}[G_N(\mathbf{r} \mid \mathbf{r}',\omega)]\, \mathcal{F}[u_z(\mathbf{r}',\omega)]\,] \qquad (3)$$

where $\mathcal{F}$ and $\mathcal{F}^{-1}$ are, respectively, direct and inverse Fourier transform in spatial domain.

Acoustic pressure backward source plane can then be propagated by multiplying wave number spectrum of normal particle velocity with spatial Fourier transform of a real velocity-to-pressure propagator $G_{up}^{propagation}$:

$$G_{up}^{propagation}(\mathbf{r} \mid \mathbf{r}',\omega) = -i\rho\omega\, G_N(\mathbf{r} \mid \mathbf{r}',\omega) \qquad (4)$$

Note that the $e^{-i\omega t}$ time convention is used.

2.2 Velocity-based NAH in moving fluid medium

As velocity-based NAH in static fluid medium is based on first Rayleigh's integral formula, velocity-based NAH in moving fluid medium is based on convective first Rayleigh's integral formula. This formula can be derived from convective Kirchhoff-Helmholtz integral formula in the case of a mean flow $\mathbf{U} = U\mathbf{x}$ parallel to the hologram plane (x', y') [11]:

$$p(\mathbf{r},\omega) = -\iint_S G_{N_\beta}(\mathbf{r} \mid \mathbf{r}',\omega)\partial p(\mathbf{r}',\omega)/\partial z\, dx'dy' \qquad (5)$$

$$\text{with} \begin{cases} G_{N_\beta}(\mathbf{r} \mid \mathbf{r}',\omega) = e^{ik(r_\beta - M(x-x'))/\beta^2}/2\pi r_\beta \\ r_\beta = \sqrt{(x-x')^2 + \beta^2[(y-y')^2 + (z-z')^2]} \end{cases}$$

where $M = U/c$ is the Mach number of the flow, c the speed of sound and $\beta = \sqrt{1-M^2}$.

Acoustic pressure at $\mathbf{r}$ can be evaluated from normal acoustic pressure gradient on surface S by means of convective Neumann Green's function G_{N_β}. This Green's function can be derived from convective free-space Green's function using the image's source method [11]. Note that these formulas are written for uniform subsonic mean flows.

As for static case, convective Euler's equation can be used to express normal pressure gradient in terms of normal particle velocity:

$$\partial p(\mathbf{r}',\omega)/\partial z = -\rho c\,(\,-ik + M\partial/\partial x\,)\, u_z(\mathbf{r}',\omega) \qquad (6)$$

NAH in moving fluid medium uses then two-dimensional spatial Fourier transform of Eq. (5):

$$p(\mathbf{r},\omega) = \mathcal{F}^{-1}[\rho c(-ik+M\partial/\partial x)\mathcal{F}[G_{N_\beta}(\mathbf{r} \mid \mathbf{r}',\omega)]\mathcal{F}[u_z(\mathbf{r}',\omega)]] \qquad (7)$$

Acoustic pressure backward source plane can then be propagated by multiplying wave number spectrum of normal particle velocity with spatial Fourier transform of a real convective velocity-to-pressure propagator $G_{up_\beta}^{propagation}$:

$$G_{up_\beta}^{propagation}(\mathbf{r} \mid \mathbf{r}',\omega) = \rho c\,(\,-ik + M\partial/\partial x\,)\, G_{N_\beta}(\mathbf{r} \mid \mathbf{r}',\omega) \qquad (8)$$

Note that taking $U = 0$ in precedent equations gives equations of static case.

2.3 Real convective velocity-to-pressure propagator for reconstruction

Using propagator defined in previous section (Eq. (8)), two operations can be performed:

- *propagation* ($\forall \mathbf{r} \geq \mathbf{r}'$) :

$$u_z(\mathbf{r}',\omega) \xrightarrow{\mathcal{F}[G_{up_\beta}^{propagation}(\mathbf{r}|\mathbf{r}',\omega)]} p(\mathbf{r},\omega)$$

- *reconstruction* ($\forall \mathbf{r} < \mathbf{r}'$) :

$$p(\mathbf{r}',\omega) \xrightarrow{\mathcal{F}[1/G_{up_\beta}^{propagation}(\mathbf{r}|\mathbf{r}',\omega)] = \mathcal{F}[G_{pu_\beta}^{reconstruction}(\mathbf{r}|\mathbf{r}',\omega)]} u_z(\mathbf{r},\omega)$$

Direct form of propagator $G_{up_\beta}^{propagation}$ allows propagation (backward source plane) whereas inverse form of propagator $1/G_{up_\beta}^{propagation}$ gives real convective pressure-to-velocity propagator $G_{pu_\beta}^{reconstruction}$ allowing reconstruction (toward source plane). Thus there are no real convective velocity-to-pressure propagator for reconstruction.

However, combining velocity-to-pressure propagator for propagation and pressure-to-pressure propagator for reconstruction, real convective velocity-to-pressure propagator for reconstruction can be derived [11]:

$$u_z(\mathbf{r}',\omega) \xrightarrow[transformation]{\mathcal{F}[G_{up_\beta}^{propagation}(\mathbf{r}'|\mathbf{r}',\omega)]} p(\mathbf{r}',\omega) \xrightarrow[reconstruction]{\mathcal{F}[1/G_{pp_\beta}^{propagation}(\mathbf{r}|\mathbf{r}',\omega)]} p(\mathbf{r},\omega)$$

Velocity-to-pressure propagator for propagation $G_{up_\beta}^{propagation}$ is first used to transform velocity into pressure in the hologram plane, and then pressure-to-pessure propagator for reconstruction $1/G_{pp_\beta}^{propagation}$ is used to reconstruct pressure toward source plane.

Thus propagator used in the following is the result of this combination:

$$G_{up_\beta}^{reconstruction}(\mathbf{r} \mid \mathbf{r}',\omega) = G_{up_\beta}^{propagation}(\mathbf{r}' \mid \mathbf{r}',\omega)/G_{pp_\beta}^{propagation}(\mathbf{r} \mid \mathbf{r}',\omega) \qquad (9)$$

with real convective pressure-to-pressure propagator given by [11]:

$$G_{pp_\beta}^{propagation}(\mathbf{r} \mid \mathbf{r}',\omega) = (\beta^2 - ikr_\beta)(z-z')\, e^{ik(r_\beta - M(x-x'))/\beta^2}/2\pi r_\beta^3 \qquad (10)$$

3 Simulation study

In this section, the velocity-based NAH procedure in moving fluid medium at subsonic and uniform velocity described above is tested numerically. As the aim of this work is to apply this new method at aeroacoustic sources characterization in wind tunnel, this part is focused on reconstruction in source plane of monopole and dipole sources radiating in various uniform subsonic flows.

Normal particle velocity u_z and its derivative along the flow direction $\partial u_z/\partial x$ are calculated in the hologram plane to perform NAH reconstruction using real convective velocity-to-pressure propagator (see 2.3).A virtual hologram array (x, y) of dimensions $0.45 * 0.45m^2$ with $16 * 16$ points, corresponding to $\Delta_x = \Delta_y = 0.03m$, is placed at a distance $z_H = 0.05m$ to the source plane defined by $z = 0$. To reduce wrap-around errors, zero padding is applied to reconstructed fields in spectral space.

3.1 Monopole sources

First, the simple case of a monopole source radiating in a uniform flow in positive x direction is studied. In order to simulate this kind of source the velocity potential Φ of such a source [13] is used:

$$\Phi(\mathbf{r}, \omega) = A\ e^{ik(r_\beta - M(x-x'))/\beta^2}/4\pi r_\beta \tag{11}$$

where A is a constant.
This velocity potential is linked to acoustic pressure and normal particle velocity by the following relations:

$$p(\mathbf{r}, \omega) = -\rho c\,(-ik + M\partial/\partial x)\ \Phi(\mathbf{r}, \omega) \tag{12}$$

$$u_z(\mathbf{r}, \omega) = \partial\Phi(\mathbf{r}, \omega)/\partial z \tag{13}$$

The effect of uniform flow on monopole's acoustic pressure radiation (Eq. (11) & (12)) is shown in Figure 1 for A real. The monopole's wavelength is reduced upstream and increased downstream, and its magnitude is modified by the mean flow.

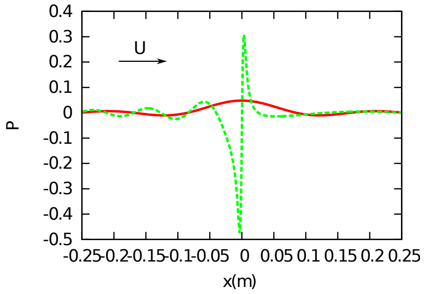

Figure 1: Real part of pressure along x for a monopole at $\mathbf{r}' = 0$ radiating at $f = 2kHz$ without flow (full line) and in a uniform flow at $M_x = 0.5$ (dashed line)

Figure 2 shows pressure levels in source plane reconstructed by NAH (bottom) compared to those obtained by theory using Eq. (12) (top) for several Mach numbers $M_x = [0; 0.25; 0.5; 0.75]$. The studied case is the following one: a monopolar potential situated at $\mathbf{r} = 0$ radiates at $2kHz$ with $A = 10^3$. Results are in good agreement with theory for all subsonic flows but windowing effects appeared for $M_x \geq 0.75$.

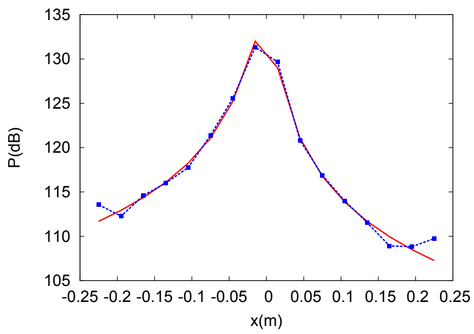

Figure 3: Reconstructed acoustic pressure level in source plane along x obtained by the theory (full line) and NAH (dashed line with points) for $M_x = 0.25$ and $f = 2kHz$

In order to compare results more accurately corresponding pressure levels along x and at $y = 0$ are shown in Figure 3 in the case of $M_x = 0.25$. Localisation and level of source are well determined: the monopole's acoustic radiation is shifted upstream by the mean flow.

Figure 4 shows pressure levels in source plane reconstructed by NAH (bottom) compared to those obtained by theory using Eq. (12) (top) for three monopole sources. The studied case is the following one: monopolar potentials situated at $\mathbf{r_1} = (0.05; 0; 0.03)$, $\mathbf{r_2} = (-0.07; 0; -0.03)$ and $\mathbf{r_3} = (0; 0; 0.1)$ radiate at $2kHz$ with $A = 10^3$. It can be seen that the present method gives also good results in such a complex sources combination.

Similar results have been found at the other frequencies allowed by hologram's array geometry: $[1-5]kHz$.

3.2 Dipole sources

Then, the case of a dipole source of axis x radiating in a uniform flow in positive x direction is studied. In order to simulate this kind of source the velocity potential Φ of such a source is derived using the image's source method:

$$\Phi(\mathbf{r}, \omega) = A((1 - ikr_\beta/\beta^2)(x - x') + ikMr_\beta^2/\beta^2)\ e^{ik(r_\beta - M(x-x'))/\beta^2}/4\pi r_\beta^3 \tag{14}$$

Acoustic pressure and normal particle velocity of the convective dipole source can be obtained from Eq. (12) & (13).

The effect of uniform flow on dipole's acoustic pressure radiation (Eq. (12) & (14)) is shown in Figure 5 for A real. The dipole's wavelength is reduced upstream and increased downstream, and its magnitude is modified by the mean flow.

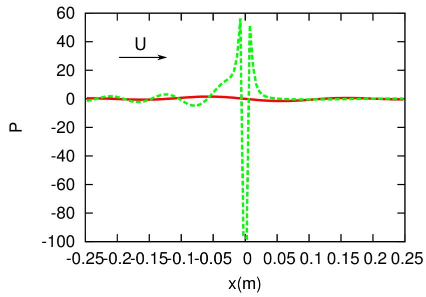

Figure 5: Real part of pressure along x for a dipole at $\mathbf{r}' = 0$ radiating at $f = 2kHz$ without flow (full line) and in a uniform flow at $M_x = 0.5$ (dashed line)

Figure 6 shows pressure levels in source plane reconstructed by NAH (bottom) compared to those obtained by theory using Eq. (12) (top) for several Mach numbers $M_x = [0; 0.25; 0.5; 0.75]$. The studied case is the following one: a dipolar potential situated at $\mathbf{r} = 0$ radiates at $2kHz$ with $A = 10^3$. Results are in good agreement with theory for all subsonic flows but windowing effects appear for $M_x \geq 0.5$.

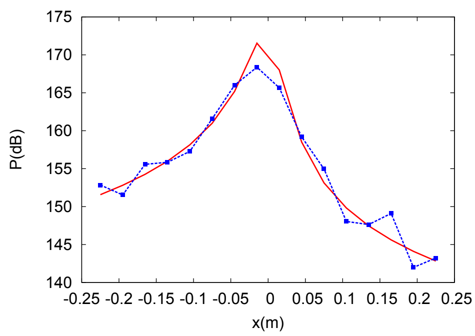

Figure 7: Reconstructed acoustic pressure level in source plane along x obtained by the theory (full line) and NAH (dashed line with points) for $M_x = 0.25$ and $f = 2kHz$

In order to compare results more accurately corresponding pressure levels along $x$and at $y = 0$ are shown in Figure

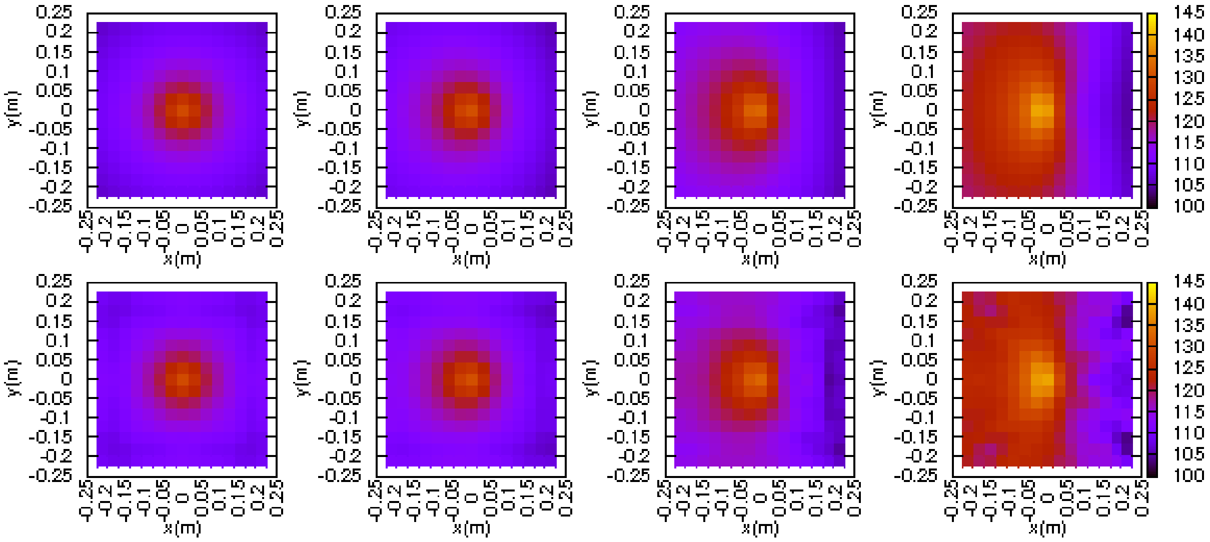

Figure 2: Reconstructed acoustic pressure level in source plane obtained by the theory (top) and NAH (bottom) for $M_x = [0; 0.25; 0.5; 0.75]$ and $f = 2kHz$.

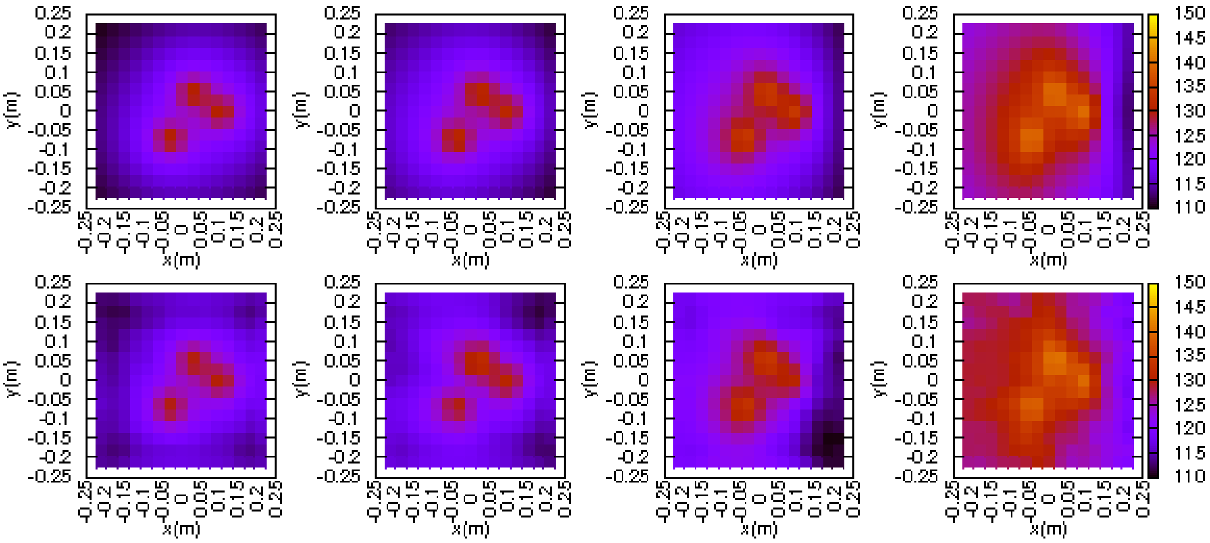

Figure 4: Reconstructed acoustic pressure level in source plane obtained by the theory (top) and NAH (bottom) for $M_x = [0; 0.25; 0.5; 0.75]$ and $f = 2kHz$.

7 in the case of $M_x = 0.25$. The source is well localized but levels are slightly under-estimated ($\sim 2dB$) at source location due to high pressure variations at this location. It can be seen that the dipole's acoustic radiation is also shifted upstream by the mean flow.

Similar results have been found at the other frequencies allowed by hologram's array geometry: $[1 - 5]kHz$.

Note that all results presented in this section are obtained without any regularization method. Thus velocity-based NAH seems to be more robust than pressure-based NAH. This has been already noticed by Jacobsen & al. in [12].

4 Conclusion

This paper presents a new non-intrusive method to characterize aeroacoustic sources in wind tunnel. This method is based on rewriting NAH using convective Rayleigh's first integral formula. In this way, one can obtain a NAH procedure applicable in uniform subsonic flows using real-space propagators built on the convective Green's function. Thus acoustic field can be reconstructed towards sources using a convective velocity-to-pressure propagator applied at velocity measurements in an hologram plane parallel to the flow.

Numerical study shows that this method is relevant in the case of classical aeroacoustic sources (combinations of monopoles and dipoles) radiating at various subsonic Mach numbers and frequencies. Indeed, reconstructed acoustic fields allow a good localization and quantification of maximal pressure magnitude without any additional inverse method or hypothesis on sources. However, acoustic pressure level at source location is slightly underestimated in the case of dipole sources and windowing effects appear at high subsonic Mach numbers. These problems could be avoided using regularization methods [8].

In order to confirm the efficiency of this method, experiments will be performed in wind tunnel with a flush-mounted loudspeaker simulating a convective monopole source. Laser Doppler Velocimetry (LDV) will be used to obtain hologram measurements of normal particle velocity component [13] without disturbances created by flow-measurement array interaction.

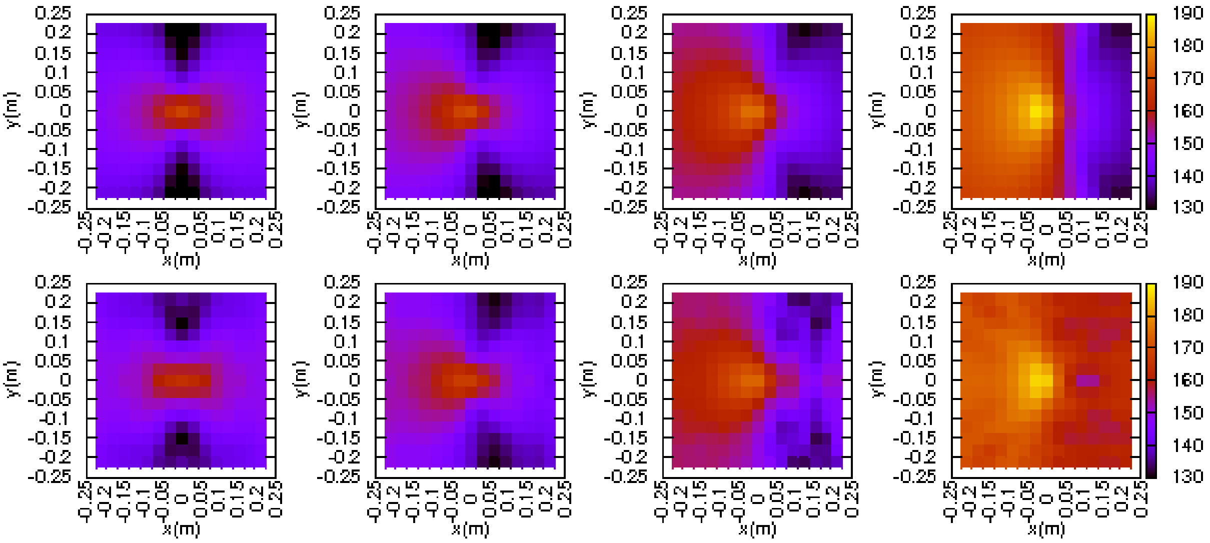

Figure 6: Reconstructed acoustic pressure level in source plane obtained by the theory (top) and NAH (bottom) for $M_x = [0; 0.25; 0.5; 0.75]$ and $f = 2kHz$.

References

[1] H. V. Fuchs, "On the application of acoustic mirror, telescope and polar correlation techniques to jet noise source location", *J. Sound Vib.* **58**, 117-126 (1978)

[2] U. Michel, "History of acoustic beamforming", *1st Berlin Beamforming Conference (BeBeC)* (2006)

[3] R. P. Dougherty, *Beamforming in acoustic testing*, Part. 2 in Aeroacoustic Measurements, edited by T. Mueller, Springer-Verlag Berlin Heidelberg, New York (2002)

[4] T. Brooks, W. Humphreys, "Deconvolution Approach for the Mapping of Acoustic Sources (DAMAS) Determined from Phased Microphone Arrays", *10th AIAA/CEAS Aeroacoustics Conference* (2004)

[5] T. Padois, C. Prax, V. Valeau, "Potentiality of time-reversed array processing for localizing acoustic sources in flows", *3rd Berlin Beamforming Conference (BeBeC)* (2010)

[6] J. D. Maynard, E. G. Williams, Y. Lee, "Nearfield acoustic holography: I. Theory of generalized holography and the development of NAH", *J. Acoust. Soc. Am.* **78**, 1395-1412 (1985)

[7] W. A. Veronesi, J. D. Maynard, "Nearfield acoustic holography (NAH): II. Holographic reconstruction algorithms and computer implementation", *J. Acoust. Soc. Am.* **81**, 1307-1322 (1987)

[8] E. G. Williams, "Regularization methods for near-field acoustical holography", *J. Acoust. Soc. Am.* **110**(4), 1976-1988 (2001)

[9] R. J. Ruhala, D. C. Swanson, "Planar near-field acoustical holography in a moving medium", *J. Acoust. Soc. Am.* **112**(2), 420-429 (2002)

[10] H-S. Kwon, Y. Niu, Y-J. Kim, "Planar nearfield acoustical holography in moving fluid medium at subsonic and uniform velocity", *J. Acoust. Soc. Am.* **128**(4), 1823-1832 (2010)

[11] H. Parisot-Dupuis, F. Simon, E. Piot, "Aeroacoustic sources localization by means of nearfield acoustic holography adapted to wind tunnel conditions", *Inter-noise*, Osaka (2011)

[12] F. Jacobsen, Y. Liu, "Near field acoustic holography with particule velocity transducers", *J. Acoust. Soc. Am.* **118**(5), 3139-3144 (2005)

[13] E. Piot, F. Micheli & F. Simon, "Optical acoustic pressure measurements in a large-scale test facility with mean flow", *16th AIAA/CEAS Aeroacoustics Conference* (2010)